

Frequency shift of optical phonons in doped graphene layers

Srijan Kumar Saha¹, U. V. Waghmare², H. R. Krishnamurthy^{1,2} and A. K. Sood¹

¹*Department of Physics, Indian Institute of Science, Bangalore 560012, India*

²*Theoretical Sciences Unit, Jawaharlal Nehru Centre for Advanced Scientific Research, Bangalore 560064, India*

(Dated: February 8, 2020)

We use first-principles density-functional calculations to determine the frequency shift of the A'_1 - \mathbf{K} phonon (Raman D band) in monolayer graphene, as a function of the charge doping. A detailed DFT study on the electron-phonon coupling and the phonon line width of E_{2g} - Γ and A'_1 - \mathbf{K} phonons are also performed for graphene multi-layers. Furthermore, we explain the experimentally observed '1/(Number of Layers)' behaviour of the Raman G band position after including the dynamic response treated within time dependent perturbation theory.

PACS numbers: 71.15.Mb, 63.20.Kr, 78.30.Na, 81.05.Uw

Graphene, a two-dimensional honeycomb lattice of sp^2 -bonded carbon atoms [1], is known to exhibit many remarkable properties that are of fundamental interest and technological relevance. Being the fundamental building block for carbon allotropes of other dimensionality, it can be stacked into 3d graphite or rolled into 1d nanotube. Graphene has created a great interest in the scientific community due to its excellent mechanical and electronic characteristics, scalability to nanometer sizes [2] and easy accessibility to optical probes. Moreover, this atomically-thin sheet is thermodynamically stable, continuous on a macroscopic scale and exhibits high crystal quality. A very intriguing feature of graphene is related to the fact that its electron transport is essentially governed by the Dirac's (relativistic) equation and can be controlled externally [3, 4, 5, 6]. Using electric field in an FET geometry it is possible to dope graphene layers by changing the carrier concentration in the samples. In particular, its phonon spectrum can be modified significantly by tuning the applied gate voltage [7, 8].

Phonon dispersions of graphene exhibit two Kohn anomalies in the highest optical branches at Γ and \mathbf{K} (E_{2g} mode - Raman G band and A'_1 mode - Raman D band, respectively). The electron phonon couplings for these modes are particularly large and negligible for all the other modes at Γ and \mathbf{K} [9]. In this paper, we calculate the frequency shift of the long wavelength optical phonon (E_{2g} - Γ mode) in graphene as a function of the number of layers. Phonon line width and the electron phonon coupling (EPC) for the above two optical phonons are also extensively studied in graphene multi-layer. Furthermore, for the first time, we compute the variation of phonon frequency of the A'_1 mode at \mathbf{K} in a graphene monolayer, as a function of doping concentration. Calculations are done first using a fully ab-initio approach within the standard Born-Oppenheimer approximation and then time-dependent perturbation theory is used to explore the effect of dynamic response.

Our ab-initio calculations are performed using density functional theory (DFT) [10] in the generalized gradient approximation. We have used the PWSCF [11]

implementation of DFT, with Perdew-Burke-Ernzerhof (PBE) [12] for the exchange correlation functional and ultrasoft pseudo potential [13] to represent the interaction between ionic cores and valence electrons. Kohn-Sham wave functions are represented with a plane wave basis truncated at an energy cut off of 40 Ry. The two-dimensional graphene crystal is simulated using a supercell geometry with a vacuum of 7.5 Å in the z-direction to ensure negligible interaction between its periodic images. The Brillouin zone integration is done on a uniform $36 \times 36 \times 1$ Monkhorst-Pack [14] grid. An electron smearing of 0.02 Ry with Fermi-Dirac distribution is used to accelerate the slow convergence of self-consistent calculation in graphene layers by smoothing out the discontinuities present in the Fermi distribution at zero temperature. Structural relaxation is carried out in each case to minimize the forces acting on each of the atoms using Broyden-Fletcher-Goldfarb-Shanno (BFGS) based method [15]. Phonon frequencies and electron phonon couplings are calculated using Density Functional Perturbation Theory (DFPT) [16] at the level of linear response, which allows the exact (within DFT) computations of phonon frequencies at any Brillouin zone point. The Fermi-energy shift with doping is simulated by considering an excess electronic charge which is compensated by a uniformly charged back-ground.

In graphene, the Fermi surface is reduced to two equivalent \mathbf{K} and \mathbf{K}' points in opposite corners of the 2D hexagonal Brillouin zone where the valence and conduction bands touch each other. This leads to the Dirac cone spectrum $\epsilon_{\pi^*/\pi}(\mathbf{K}+\mathbf{k}) = \pm \hbar v_F k$ for the π^* and π bands, where v_F is the Fermi velocity of the massless (2+1) dimensional Dirac fermions and \mathbf{k} is a small vector. Within this approximation, at zero temperature ($T = 0$ K), the layer charge concentration and the Fermi energy are related via

$$\sigma = \text{sign}(\epsilon_F) \frac{\epsilon_F^2}{\pi(\hbar v_F)^2} = \text{sign}(\epsilon_F) \epsilon_F^2 \times 10.4 \times 10^{13} \text{ cm}^{-2} (\text{eV})^{-2} \quad (1)$$

where $\hbar v_F = 5.53 \text{ eV} \cdot \text{Å}$ from our DFT calculation, in

excellent agreement with the previous DFT result [17] and $\epsilon_F = 0$ at the π bands crossing (known as Dirac point). For very small doping concentration (order of 10^{13}cm^{-2}), the linearized bands are a good approximation. We have used this model of strongly interacting two-dimensional Dirac fermions in few layer- graphene as an approximation because the Dirac singularity is the topological property of the electronic spectra that should be stable towards the weak 3d inter-layer coupling even in few layer- graphene. That's why the Fermi velocity for the few layers of graphene [18] is taken to be the same as for a single layer within a good approximation for low doping concentration. To check validity of the above approximation in graphene multi-layers, we have performed the DFT calculations of the electronic band structure for monolayer, bilayer, trilayer and tetralayer graphene and our results (Figure 1) confirm that the above assumption is justified.

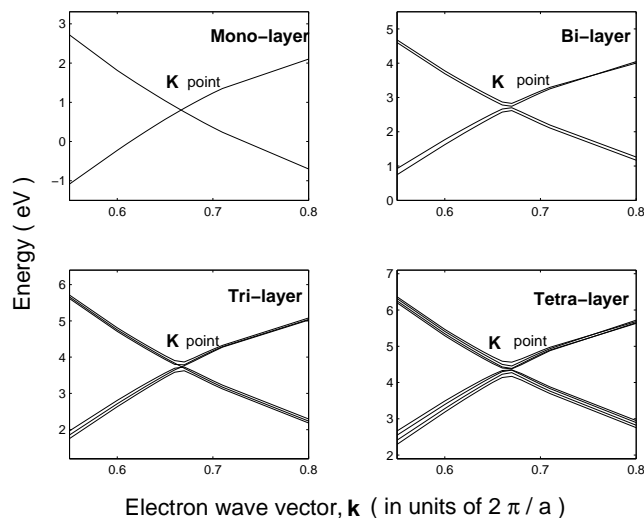


FIG. 1: The electronic band structure of graphene layers determined with ab-initio DFT calculations.

We first determine the total energy and electronic density by solving the self-consistent Kohn-Sham equations for the equilibrium crystal geometry where the relative atomic positions in the unit cell yield zero forces and lattice parameters lead to a zero stress-tensor. Once the unperturbed ground state is determined, phonon frequencies are obtained by using DFPT which calculates the linear response of the electrons to a static perturbation induced by ionic displacements. This approach is based on the adiabatic (also referred to as the Born-Oppenheimer or static) approximation. At zero-doping, our computed $E_{2g}-\Gamma$ and $A'_1-\mathbf{K}$ phonon frequencies in a monolayer graphene are $\omega_{\Gamma}^{static}(0) = 1553.3 \text{ cm}^{-1}$ and $\omega_{\mathbf{K}}^{static}(0) = 1301.7 \text{ cm}^{-1}$, respectively. Infact, the phonon exactly at the \mathbf{K} point is not the relevant one for the Raman D or 2D bands in graphene; rather what is relevant is the phonon at $(\mathbf{K} - \Delta\mathbf{K})$ where $\Delta\mathbf{K}$ is deter-

mined by the double resonance process [19, 20, 21]. For the typical experimentally used laser excitation of 2.41 eV, the value of $\Delta\mathbf{K}$ is 0.0855 (in units of $2\pi/a$). Our results of the frequency shifts for the \mathbf{K} point phonon ($\Delta\omega_{\mathbf{K}}^{static}$) and the $(\mathbf{K} - \Delta\mathbf{K})$ point phonon ($\Delta\omega_{\mathbf{K}-\Delta\mathbf{K}}^{static}$) with charge doping σ are shown in Figure 2. In both panels, the open circles show the results obtained when the lattice spacing is kept fixed at its value corresponding to the undoped case and the filled stars show the results obtained when the lattice spacing is optimized for each doping concentration. The optimization leads to a lattice expansion with electron doping and a lattice contraction with hole doping, and gives substantial change in the phonon frequency shift. Interestingly, Figure 2 shows that the frequency shift of the $A'_1-\mathbf{K}$ phonon on the charge doping in a graphene monolayer is very different compared to the Γ point phonon [17].

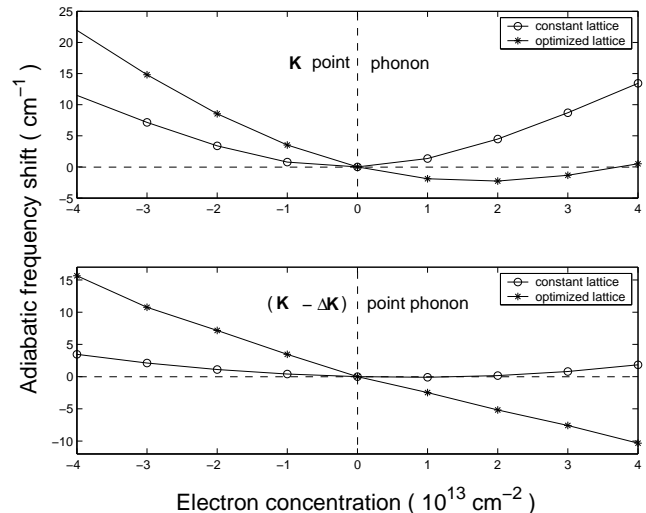


FIG. 2: Adiabatic frequency shift of the \mathbf{K} - A'_1 and $\mathbf{K} - \Delta\mathbf{K}$ phonon in graphene monolayer as a function of charge doping σ , with respect to the zero-doping frequency.

Within the adiabatic approximation, above results are generically expected on physical grounds. For the long-wavelength Γ phonon (small wave-vector \mathbf{q}), a high density of electron doping leads to an effective screening of the ion-ion interactions, reducing the elastic coupling in the lattice and hence leading to a softening of the phonons. On the other hand, in the case of the \mathbf{K} -point phonon with a larger wave-vector which connects two points in the Fermi surface, electrons are no longer able to effectively shield the ion-ion interactions and the vibrational properties shows a giant and sharp Kohn-anomaly - a precipitous phonon softening at \mathbf{K} point. With doping, the change in the Fermi surface moves that Kohn-anomaly away from $\mathbf{q} = \mathbf{K}$ and stiffens \mathbf{K} -point phonon (Figure 2).

So far we have used the standard adiabatic approximation which is usually justified in ordinary metals where

the electronic energy gap between the ground and the excited states is larger than the phonon energy so that the phonons respond to a time averaged electron distribution. In graphene, however, this approximation is inadequate because of its unique massless Dirac-like electron band dispersion and comparable electronic and phonon energy scale. The complete break-down of the adiabatic approximation in doped graphene has been recently demonstrated, both theoretically and experimentally [7, 17]. Hence, for single-, double- and few layer- doped graphene, we next consider the phonon as a dynamic perturbation treated within time-dependent perturbation theory.

Using such a dynamic approach in the context of DFT, the self-energy of a phonon mode ν at wave-vector \mathbf{q} can be written as [22],

$$S_\nu(\mathbf{q}, \omega_{\mathbf{q}\nu}) = \frac{2}{N_k} \sum_{\mathbf{k}, i, j} |g_{(\mathbf{k}+\mathbf{q})i, \mathbf{k}j}^\nu|^2 \frac{f_{(\mathbf{k}+\mathbf{q})i} - f_{\mathbf{k}j}}{\epsilon_{(\mathbf{k}+\mathbf{q})i} - \epsilon_{\mathbf{k}j} - \hbar\omega_{\mathbf{q}\nu} - i\eta} \quad (2)$$

where N_k is the number of \mathbf{k} -points, the sum is over $\mathbf{k} \in$ Brillouin zone, $f_{\mathbf{k}j}$ is the Fermi distribution function, η is a small real number and $g_{(\mathbf{k}+\mathbf{q})i, \mathbf{k}j}^\nu$ is the electron-phonon matrix element. Within DFPT, the electron phonon matrix element can be obtained from the first order derivative of the self-consistent Kohn-Sham potential, with respect to the atomic displacements as: $g_{(\mathbf{k}+\mathbf{q})i, \mathbf{k}j}^\nu = \langle (\mathbf{k} + \mathbf{q})i | \delta V_{KS} / \delta u_{\mathbf{q}\nu} | \mathbf{k}j \rangle / \sqrt{2M\omega_{\mathbf{q}\nu}}$ where $u_{\mathbf{q}\nu}$ is the amplitude of the displacement of the phonon ν of wave vector \mathbf{q} , $\omega_{\mathbf{q}\nu}$ its phonon frequency, M is the atomic mass, V_{KS} the Kohn-Sham potential and $|\mathbf{k}j\rangle$ is a Bloch eigenstate with wave-vector \mathbf{k} , band index j and energy $\epsilon_{\mathbf{k}j}$.

The dynamic correction to the energy shift arising from the electron-phonon interaction is given by the real part of the phonon self-energy as:

$$\frac{\hbar\Delta\omega_{\mathbf{q}}}{2} = \frac{2}{N_k} \sum_{\mathbf{k}, i, j} |g_{(\mathbf{k}+\mathbf{q})i, \mathbf{k}j}^\nu|^2 \mathcal{P} \left[\frac{f_{(\mathbf{k}+\mathbf{q})i} - f_{\mathbf{k}j}}{\epsilon_{(\mathbf{k}+\mathbf{q})i} - \epsilon_{\mathbf{k}j} - \omega_{\mathbf{q}\nu}} \right] \quad (3)$$

where \mathcal{P} takes the principal part of its argument.

The phonon line width (FWHM) is twice the imaginary part of $S_\nu(\mathbf{q}, \omega_{\mathbf{q}\nu})$ and can also be obtained from the Fermi golden rule [23]:

$$\gamma_{\mathbf{q}\nu} = \frac{4\pi}{N_k} \sum_{\mathbf{k}, i, j} |g_{(\mathbf{k}+\mathbf{q})i, \mathbf{k}j}^\nu|^2 (f_{\mathbf{k}j} - f_{(\mathbf{k}+\mathbf{q})i}) \delta(\epsilon_{(\mathbf{k}+\mathbf{q})i} - \epsilon_{\mathbf{k}j} - \omega_{\mathbf{q}\nu}) \quad (4)$$

Ideally, in the dynamic case, ω should be determined self-consistently. However, considering the dynamic and doping effects as perturbation, at the lowest order, we can use the adiabatic undoped phonon frequency ω_0^{static} in place of ω . For \mathbf{q} near Γ -point, we can also consider the electron phonon coupling as $|g_{(\mathbf{K}+\mathbf{k})j, (\mathbf{K}+\mathbf{k})i}|^2 = \langle g_{\Gamma}^2 \rangle_{\mathbf{F}} [1 \pm \cos(2\theta)]$, where θ is the angle between the phonon-polarization \mathbf{q} and \mathbf{k} , the sign \pm depends on the

transition and $\langle g_{\Gamma}^2 \rangle_{\mathbf{F}} = \sum_{i,j} |g_{\mathbf{K}i, \mathbf{K}j}|^2 / 4$, the sum is for the two degenerate π bands at $\epsilon_{\mathbf{F}}$ (see Eqn. 6 and note 24 of Ref. [9]).

Based on the above approximations with the linear electron dispersion near Dirac point, we find that the change of Raman G-band phonon energy at zero temperature can be described as,

$$\hbar\Delta\omega_{\Gamma}^{dynamic} = \alpha_{\Gamma} |\epsilon_{\mathbf{F}}| + \frac{\alpha_{\Gamma} \hbar\omega_{\Gamma}^{static}(0)}{4} \ln \left| \frac{2|\epsilon_{\mathbf{F}}| - \hbar\omega_{\Gamma}^{static}(0)}{2|\epsilon_{\mathbf{F}}| + \hbar\omega_{\Gamma}^{static}(0)} \right| \quad (5)$$

where $\alpha_{\Gamma} = \frac{2A_0 \langle g_{\Gamma}^2 \rangle_{\mathbf{F}}}{\pi \hbar^2 v_F^2}$, $A_0 = 5.23 \text{ \AA}^2$ is the equilibrium unit cell area. In this case, the energy shift diverges logarithmically when the magnitude of the Fermi energy becomes the half of the phonon energy and increases in proportion to the Fermi energy for $|\epsilon_{\mathbf{F}}| > \hbar\omega_0^{static}/2$ as long as the effect of the charge doping can be considered as a perturbation. Beyond this, one can easily notice a considerable change in α_{Γ} and ω_{Γ}^{static} with charge doping.

In order to calculate the dynamic frequency shift of Raman G band for graphene layers, we need α_{Γ} for different layers. This is calculated using ab-initio density functional theory and results are given in Table I. Further, we find that the static zero-doping frequencies $\omega_{\mathbf{K}}^{static}(0) = 1301.7 \text{ cm}^{-1}$ and $\omega_{\Gamma}^{static}(0) = 1553.3 \text{ cm}^{-1}$ do not change with the number of graphene layers, n . We plot the dynamic frequency shift of the Raman G band as a function of the charge doping for different graphene layers in Figure 3(a). One can readily notice (from Figure 2) that for small doping (around $0.4 \times 10^{-13} \text{ cm}^{-2}$) expected in zero-biased unintentionally doped graphene on a substrate, the static frequency shift is very small and can be treated as a correction ($< 1 \text{ cm}^{-1}$) with respect to the dynamic one. For such a low doping concentration, the dynamic shift shows a linear dependence on $1/n$ (Figure 3(b)). Interestingly, this is very similar to the the experimentally observed [24] dependence of the the Raman G band position on the number of layers. We, therefore, suggest that the frequency shift of the Raman G mode on the number of layers is dominantly due to the unintentional charge doping which can be understood based on the dynamic effects.

Moreover, our DFT calculations (Table I) show that the phonon linewidth changes very little with the number of graphene layers. This result is expected on physical grounds. In graphene layers, the phonon linewidth due to the electron phonon coupling obtained from the imaginary part of the phonon self-energy (or equivalently from the Fermi Golden rule) is [7, 17]

$$(\gamma_{\Gamma})_n = \frac{\pi (\alpha_{\Gamma})_n n \hbar\omega_0^{static}}{2} [f(-\hbar\omega_0^{static} - 2\epsilon_{\mathbf{F}}) - f(\hbar\omega_0^{static} - 2\epsilon_{\mathbf{F}})] \quad (6)$$

where n is the number of graphene layers. We find that $(\alpha_{\Gamma})_n n$ is almost constant with the number of layers,

Number of Layers, n	α		$\gamma[T = 0K] (cm^{-1})$	
	α_{Γ}	$\alpha_{\mathbf{K}}$	γ_{Γ}	$\gamma_{\mathbf{K}}$
1	4.441×10^{-3}	13.33×10^{-3}	11.70	8.10
2	2.223×10^{-3}	6.68×10^{-3}	11.56	8.04
3	1.457×10^{-3}		11.43	
4	1.085×10^{-3}		11.32	
5	0.889×10^{-3}		11.23	

TABLE I: Electron-phonon coupling strength, α and phonon-line widths, $\gamma (cm^{-1})$ at Γ and \mathbf{K} for graphene layers. The values are computed using density functional theory. α decreases very fast with increasing number of layers while the change in γ is very small.

leading to a very small variation of phonon line width with number of layers. At zero temperature, we get $\gamma(T=0K) = \frac{\pi(\alpha_{\Gamma})_n \hbar \omega_0^{static}}{2} \Theta(\hbar \omega_0^{static} - 2|\epsilon_F|)$. It implies that the broadening is nonzero only for $|\epsilon_F| < \hbar \omega_0^{static}/2$ when the scattering process is allowed by the Pauli exclusion principle.

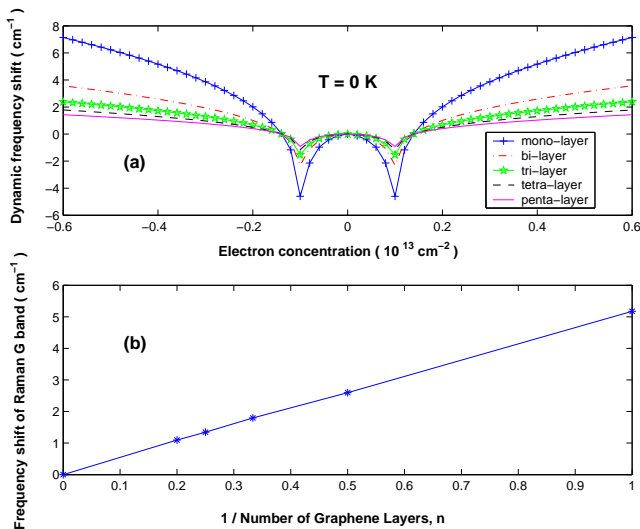


FIG. 3: (Color online) (a) Dynamic frequency shift with charge doping in graphene multi-layers and (b) Frequency shift of Raman G band as a function of the number of layers.

Finally, we discuss the effect of the charge doping on the \mathbf{K} -point phonon. Recent experimental observation [8] indicates that although the width and the peak position of the Raman G and D^* bands (second order of \mathbf{K} point phonons) exhibit similar doping dependence, the magnitudes of the changes are only around 10 percent of the G band. This small dependence suggests that for the large wave vector phonon (\mathbf{K} point phonon) there is a cancellation of the large inter-band and intra-band contribution [25] in the dynamic response and the static DFT frequency shift (see Figure 2) plays the major role. We are also studying the layer dependence of the \mathbf{K} -point frequency shift in doped graphene multi-layers and that

will be reported elsewhere very soon.

In conclusion, we have computed, from first-principles, the frequency shift of the $A'_1\text{-K}$ phonon (Raman D band) in monolayer graphene, as a function of the charge doping. A detailed DFT study on the electron-phonon coupling and the phonon line width of $E_{2g}\text{-}\Gamma$ and $A'_1\text{-K}$ phonons have also been performed for graphene multi-layers. Furthermore, we explain the experimentally observed '1/(Number of Layers)' behaviour of the Raman G band position after including the dynamic response treated within the time dependent perturbation theory.

S.K.S. gratefully acknowledges the financial support of Research Fellowship from Council of Scientific and Industrial Research (India) under Award Number 9/79(913)/2002-EMR-I. A.K.S. thanks Department of Science and Technology (India) for financial support. We also thank Prof. Prabal K Maiti for providing access to his computer resources.

- [1] K.S. Novoselov *et al.* Science **306**, 666 (2004).
- [2] Y. Zhang *et al.* Appl. Phys. Lett. **86**, 073104 (2005).
- [3] K.S. Novoselov *et al.* Nature **438**, 197 (2005).
- [4] Y. Zhang, Y.W. Tan, H.L. Stormer, and P. Kim, Nature **438**, 201 (2005).
- [5] K. S. Novoselov *et al.*, Proc. Natl. Acad. Sci. USA **102**, 10451 (2005).
- [6] K. S. Novoselov *et al.*, Nature Physics **2**, 177 (2006).
- [7] Simone Pisana *et al.* cond-mat/0611714 (2006).
- [8] J. Yan *et al.* cond-mat/0612634 (2006).
- [9] S. Piscanec, M. Lazzeri, F. Mauri, A.C. Ferrari, and J. Robertson, Phys. Rev. Lett. **93**, 185503 (2004).
- [10] P. Hohenberg, W. Kohn Phys. Rev. **136**, B864 (1964); W. Kohn and L.J. Sham Phys. Rev. **140**, A1133 (1965).
- [11] S. Baroni, S. de Gironcoli, A. Dal Corso, and P. Gianozzi, <http://www.pwscf.org>.
- [12] J.P. Perdew, K. Burke, and M. Ernzerhof Phys. Rev. Lett. **77**, 3865 (1996).
- [13] D. Vanderbilt, Phys. Rev. B **41**, 7892 (1990).
- [14] M. Methfessel and A.T. Paxton Phys. Rev. B **40**, 3616 (1989).
- [15] <http://www.library.cornell.edu/nr/bookpdf/c10-7.pdf>.
- [16] S. Baroni, S. de Gironcoli, A. Dal Corso, and P. Gianozzi, Rev. Mod. Phys. **73**, 515 (2001).
- [17] M. Lazzeri and F. Mauri, Phys. Rev. Lett. **97**, 266407 (2006).
- [18] T. Ohta *et al.* cond-mat/0612173 (2006).
- [19] C. Thomsen and S. Reich, Phys. Rev. Lett. **85**, 5214 (2000).
- [20] A.C. Ferrari *et al.* Phys. Rev. Lett. **97**, 187401 (2006).
- [21] D. Graf *et al.* Nano Lett., **7** (2), 238 -242, 2007.
- [22] For example, see, G. D. Mahan, Many Particle Physics, Third Edition, Page 140.
- [23] M. Lazzeri *et al.* Phys. Rev. B **73**, 155426 (2006).
- [24] A. Gupta *et al.* cond-mat/0606593 (2006).
- [25] A. H. Castro Neto and Francisco Guinea, Phys. Rev. B **75**, 045404 (2007).